Astron. Astrophys. 320, 776–782 (1997)

ASTRONOMY
AND
ASTROPHYSICS

Tidal radii of the globular clusters M 5, M 12, M 13, M 15, M 53, NGC 5053 and NGC 5466 from automated star counts

I. Lehmann[1] **and R.-D. Scholz**[2]

[1] Astrophysikalisches Institut Potsdam, An der Sternwarte 16, D-14482 Potsdam, Germany
[2] WIP Astronomie / Universität Potsdam, Sternwarte Babelsberg, D-14482 Potsdam, Germany

Received 12 August 1996 / Accepted 9 October 1996

Abstract. We present new tidal radii for seven Galactic globular clusters using the method of automated star counts on Schmidt plates of the Tautenburg, Palomar and UK telescopes. The plates were fully scanned with the APM system in Cambridge (UK). Special account was given to a reliable background subtraction and the correction of crowding effects in the central cluster region. For the latter we used a new kind of crowding correction based on a statistical approach to the distribution of stellar images and the luminosity function of the cluster stars in the uncrowded area. The star counts were correlated with surface brightness profiles of different authors to obtain complete projected density profiles of the globular clusters. Fitting an empirical density law (King 1962) we derived the following structural parameters: tidal radius r_t, core radius r_c and concentration parameter c. In the cases of NGC 5466, M 5, M 12, M 13 and M 15 we found an indication for a tidal tail around these objects (cf. Grillmair et al. 1995).

Key words: globular clusters: general – methods: statistical

1. Introduction

The projected radial density profile of the majority of Galactic globular clusters is well represented by a simple three-parameter model (King 1962, 1966a). The examination of the core radius r_c and the tidal radius r_t gives important information about the internal dynamics of the cluster and the influence of the Galactic tidal field. New CCD techniques made it possible to obtain reliable surface brightness data for the innermost parts (some arcmin) of the radial profile (Djorgovski et al. 1986). But since the typical angular size of a globular cluster is about 30 arcmin this method failed in the outer regions. The tidal radius r_t was then usually derived by extrapolation of the CCD data or by conventional star counts on wide-field photographic plates (King, Hedemann & Hodge 1968, Peterson 1976, Da Costa & Freeman 1976). The tidal radius r_t crucially depends on the star count method applied in the outer cluster region.

Automated star counts, for the first time used by Herzog & Illingworth (1977), increase the data quality due to a higher statistical significance in the outer cluster region. A pioneering work in this field was the examination of the stellar density as a function of position and magnitude in the southern globular cluster M 55 by Irwin & Trimble (1984) using plates of the Anglo-Australian telescope fully scanned with the APM measuring machine (Kibblewhite et al. 1984). Recently, Grillmair et al. (1995) examined the outer structure of 12 Galactic globular clusters using automated star counts obtained from UK Schmidt plates with the APM facility. Within the framework of the absolute proper motion programme (Scholz et al. 1996) seven globular clusters on different Schmidt plates were scanned by the APM. We examine these simple image mode scans to derive projected stellar density profiles applying a new luminosity-dependent crowding correction in the central cluster region. Here we discuss the tidal radii of M 5, M 12, M 13, M 15, M 53, NGC 5053 and NGC 5466 obtained from fitting empirical King profiles (King 1962) to the counts correlated with surface brightness profiles for the innermost cluster area in comparison with the new CCD results of Trager, Djorgovski & King (1993) and Trager, King & Djorgovski (1995) based on conventional star counts in the outer cluster region.

2. Observations and measurements

The plates used in this investigation were taken with the Tautenburg (134/200/400), Palomar (122/183/307) and UK Schmidt (120/180/306) telescopes. The values in parentheses give the diameters of the Schmidt corretion plate, the mirror and the focal length in cm. Table 1 lists the relevant plate parameters. All plates were scanned with the APM measuring machine in Cambridge/UK (Kibblewhite et al. 1984). For more details concerning the measuring process we refer to earlier papers of Scholz, Odenkirchen & Irwin (1993, 1994). All measured objects were classified into stars, nonstellar objects, noise images and merged objects using the standard APM software. The instrumental APM magnitudes are internally calibrated (Bunclark & Irwin 1983) so that they are almost linearly related to the standard

Table 1. Plate material

Telescope	Pass-band	Scale [$\frac{\text{arcsec}}{\text{mm}}$]	exp. [min]	Object
POSSI/O1402	U+B	67.2	12	M 5
POSSI/E1402	R	67.2	45	M 5
UKST/J5193	B_J	67.2	75	M 5
Tautbg/3433	B	51.4	25	M 5
Tautbg/3436	V	51.4	25	M 5
Tautbg/5821	V	51.4	20	M 5
Tautbg/8348	B	51.4	32	M 5
Tautbg/8353	B	51.4	29	M 5
POSSI/O155	U+B	67.2	12	M 12
POSSI/E155	R	67.2	45	M 12
UKST/J6192	B_J	67.2	65	M 12
Tautbg/8349	B	51.4	30	M 12
Tautbg/8361	B	51.4	32	M 12
POSSI/O1069	U+B	67.2	12	M 13
POSSI/E1069	R	67.2	45	M 13
Tautbg/8337	B	51.4	40	M 13
Tautbg/8340	B	51.4	35	M 13
POSSI/O298	U+B	67.2	12	M 15
POSSI/E298	R	67.2	50	M 15
Tautbg/2618	B	51.4	25	M 15
Tautbg/2657	V	51.4	25	M 15
Tautbg/7595	B	51.4	30	M 15
Tautbg/7615	B	51.4	27	M 15
Tautbg/7631	V	51.4	21	M 15
Tautbg/7633	V	51.4	27	M 15
POSSI/O80	U+B	67.2	12	M 53/NGC 5053
POSSI/E80	R	67.2	45	M 53/NGC 5053
Tautbg/8351	B	51.4	30	M 53/NGC 5053
Tautbg/8355	B	51.4	35	M 53/NGC 5053
POSSI/O86	U+B	67.2	12	NGC 5466
POSSI/E86	R	67.2	45	NGC 5466
Tautbg/8352	B	51.4	46	NGC 5466
Tautbg/8358	B	51.4	40	NGC 5466

photometric system (cf. Kharchenko, Scholz & Lehmann for the case of M 5).

As an astrometric investigation was the primary goal the measurements were carried out in standard APM image mode without the special crowded field on-line reduction of Irwin (1985). We find a large percentage of stars misclassified as non-stellar objects (galaxies or merged objects) in the cluster area which increases significantly towards the central cluster region. Within a radius of about 3-5 arcmin around the cluster center, the APM detection algorithm failed for all clusters except NGC 5053 and NGC 5466 due to very strong crowding effects on the Schmidt plates. Therefore, this very central cluster region was not used in the star counts. Special attention must be given to a reliable crowding correction in the region $r >$ 2-3 arcmin as described in section 3.2.

3. Star counts

In a first step we determined the uncorrected projected density profile for the three object classes (stellar objects, galaxies and merged objects). We measured the center coordinates of all investigated clusters on every plate as median values in the distribution of stellar objects in x and y direction. The errors of the central coordinates are in the range of 0.1 to 0.2 arcmin. The uncorrected projected density was then calculated in annuli with widths of 1 arcmin around the central coordinates. The mean radius r_e of an annulus is given by

$$r_e = [\frac{1}{2}(r_i^2 + r_{i+1}^2)]^{\frac{1}{2}}, \quad (1)$$

where r_{i+1} and r_i are the outer and inner radius of the i-th annulus, respectively. Starting at about 10 arcmin away from the cluster center, the uncorrected density profiles $f(r_e)$ increase not only for the stellar images but also for merged objects and galaxies. This is due to crowding effects and must be corrected to get a more reliable number of the stellar objects in the annuli.

3.1. Background subtraction

As the clusters are usually in the center of the plates, a large area around the cluster can be used to obtain background densities. The radial range for the calculation is chosen far enough away in order to avoid cluster members, but near enough to measure the local background. A first estimation of the background density of stellar objects, galaxies and merged objects was obtained from the uncorrected profiles. With regard to a luminosity-dependent crowding correction we calculated the background densities of each object class depending on the internal APM-magnitude (described by Bunclark & Irwin (1983)) in 0.25 mag intervals. The background per magnitude interval is the sum over the annuli

$$f(\triangle m_{\text{APM}}) = \frac{\sum_{i=j}^{N} f(\triangle m_{\text{APM}})_i}{N}, \quad (2)$$

where N is the number of annuli, j the first annulus deemed to be clear out of the cluster and $f(\triangle m_{\text{APM}})_i$ the background density of the i-th annulus. The standard deviation was assumed as the mean variation $\triangle f(\triangle m_{\text{APM}})$ of the background density per magnitude interval. The complete background value and the error per object class are

$$f_{bkg} = \sum_{\triangle m_{\text{APM}}} f(\triangle m_{\text{APM}}), \quad (3)$$

$$\triangle f_{bkg} = \sum_{\triangle m_{\text{APM}}} \triangle f(\triangle m_{\text{APM}}). \quad (4)$$

Depending on the exposure time of the plates and their sensitivity we found a relative error $\frac{\triangle f_{bkg}}{f_{bkg}}$ for stellar objects of the order of 5 - 16 % indicating no important variation of the background density around the clusters. Finally we subtracted the number of background stars from the counted stars in each annulus using Eq. (1) of King (1968) for number density.

3.2. Luminosity dependent crowding correction

The method of automated star counts requires an extensive crowding correction. Instead of the earlier corrections of King (1968) and Irwin & Trimble (1984) we developed a luminosity-dependent formalism to correct for crowding
effects in the cluster region. We combined a statistical expression for the overlap of the stellar images from Lindgren (1962) and the luminosity function of the non-crowded cluster region to obtain an additional number of stellar objects from the misclassified non-stellar objects and galaxies in the crowding region.

Our correction is based on two physical assumptions: first we assume a constant stellar mixture over the complete area of the globular cluster and hence a uniform shape of the luminosity function over the whole cluster area. Relevant mass segregation occurs only in the very central region of globular clusters (Richer & Fahlman 1989) especially for a core collapsed globular cluster like M 15. This region we cannot resolve. As a second assumption we considered the galaxies and non-stellar objects in the cluster region with APM-magnitudes 1.5 mag over the identification limit of faint objects to be overlapped single stellar images. Since all clusters in consideration are located outside the Galactic plane ($\mid b \mid > 25^o$) there is no significant crowding in the background itself on our Schmidt plates.

The crowding correction was carried out in 1 arcmin
wide annuli around the cluster center. It was assumed that the crowding effects are negligible from that annulus on where the number densities of galaxies and non-stellar objects, derived from the uncorrected star counts per APM-magnitude interval, reach the 3 σ variation of the backgro und values. At first we calculated the image size of all galaxies and non-stellar objects in the annuli corrected for overlap. An overlap of stellar images reduces the added image size A' to the measured image size A given by

$$A = A'[(1 - C_1) + \frac{1}{2}(C_1 - C_2) + \ldots + \frac{1}{j}(C_{j-1} - Cj)]. \quad (5)$$

The first term in the bracket is the fraction of single images, the second of double images and so on based on a statistical approach for finding the k-th stellar object within a radius r by n measurements (Lindgren 1962). A similar formula was used by Irwin & Trimble (1984) in their correction formalism, where they corrected directly the projected number density per annulus. The formula (5) can be rewritten to

$$A = A' \sum_{j=1}^{n} \frac{1}{j}^{n} C_{j-1}[F(r)]^{j-1}[1 - F(r)]^{n+1-j}, \quad (6)$$

where $F(r)$ is the cumulative distribution of the statistic r depending on the area πr^2 and a normalization constant α. For large n, this is reduced to

$$A \cong A' \frac{[1 - exp(-\pi n \alpha r^2)]}{\pi n \alpha r^2}. \quad (7)$$

The term $n\alpha$ represents the mean number density of all objects f_{all}. The stellar images were assumed to be circular with a radius r_s. In the cases of overlap we have $r = 2r_s$ so that with $\pi r^2 = 4\pi r_s^2 = 4 < A_{iso} >$ we obtained the correction formula:

$$A \cong A' \frac{[1 - exp(-4 f_{all} < A_{iso} >)]}{4 f_{all} < A_{iso>}}, \quad (8)$$

where $< A_{iso} >$ is the mean image size of a stellar object at the threshold isophote. The measured image size per annuli A is given by the sum of the single images

$$A = \sum_{i=1}^{N} A_i \ \text{(galaxies)} + \sum_{j=1}^{M} A_j \ \text{(merged objects)}. \quad (9)$$

The mean number density f_{all} was simply obtained from the background corrected density profile of all objects.

As the second part of the crowding correction we determined the additional number of stellar objects from the added image size A'. The basic idea is to divide each image into discrete numbers of stellar objects using the information in the globular cluster's luminosity function. Since the isophotal area A_{iso} of a single stellar image is related to its APM-magnitude we can calculate the fraction of stellar objects per magnitude interval $\triangle m_{\rm APM}$ of added image size of the stellar objects

$$R(\triangle m) = \frac{N(\triangle m_{\rm APM})}{\sum_{i=1}^{N} A_i \ \text{(stellar objects)}}, \quad (10)$$

with $N(\triangle m_{\rm APM})$ the number of stellar objects per magnitude interval defined by the luminosity function of the non-crowded cluster region. Fig. 1 shows as an example the LF of the non-crowded region on the plate t8355 (object M 53). The APM-magnitudes of the plates with different passbands were converted into B, V and R magnitudes, respectively, using photoelectric standards from different sources (Table 2). This was done in order to omit some remaining bright field stars (after the subtraction of the background) from the LF using the known

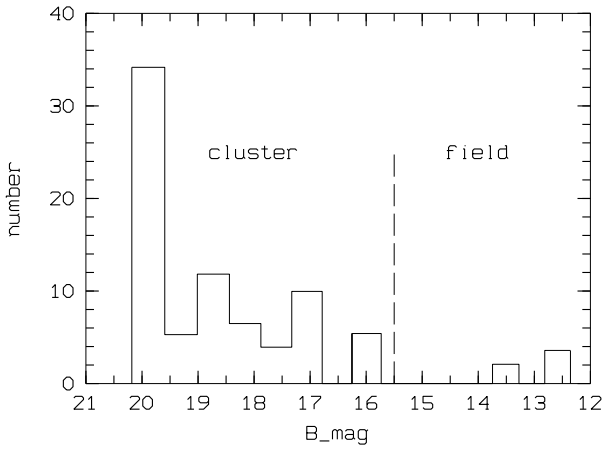

Fig. 1. Luminosity function in the uncrowded region after subtraction of the background (plate t8355, M 53). The stars on the right side of the dashed line were classified as field stars according to the known CMD of the cluster.

Table 2. Photoelectric standards and CM-diagram

cluster	standard sequence	CM-diagram
NGC 5053	Sandage & Katem (1977)	Cuffey (1965)
NGC 5466	Nemec & Harris (1987)	Cuffey (1965)
M 5	Arp (1962)	Arp (1955)
M 12	Sato et al. (1989)	Racine (1971)
M 13	Sandage (1970)	Sandage (1970)
	Baum et al. (1959)	
M 15	Sandage (1970)	Sandage (1970)
M 53	Sandage & Katem (1977)	Cuffey (1965)

CMDs of the clusters. Since we are only interested in a rough estimate, the APM magnitudes measured on the Palomar O plates (U+B) were also converted to B magnitudes.

With the fraction $R(\triangle m_{\rm APM})$ we obtained the additional number of stellar objects per magnitude interval

$$N_{add}(\triangle m) = A' R(\triangle m_{\rm APM}) \tag{11}$$

and with

$$N_{add} = \sum_{\triangle m_{\rm APM}} N_{add}(\triangle m_{\rm APM}) \tag{12}$$

the additional number of stellar objects per annulus. Then we derived the background and crowding corrected stellar density $f(r_e)$ as

$$f(r_e) = \frac{N_{stars} + N_{add} - N_{bkg}}{A} \tag{13}$$

with N_{bkg} the number of the stellar background objects. The mean error of $f(r_e)$ is caused by statistical Poisson distribution of the number of objects per area $A \sim \sqrt{N}$. The statistical error of the background was neglected due to its accurate determination over a large sky region.

The performed crowding correction leads to higher number densities in comparison to the methods of King, Hedemann & Hodge (1968) and Irwin & Trimble (1984). Nevertheless it breaks down in the very central cluster regions where the detection algorithm of the APM cannot resolve single stellar images due to strongest crowding effects on Schmidt plates.

4. Projected density profiles and the parameters r_t, r_c and c

The projected density profiles of M 5, M 12, M 13, M 15, M 53, NGC 5053 and NGC 5466 from the different plates were matched to a single profile for each cluster and correlated with surface brightness measurements from Kron & Mayall (1960), King (1966b) and Kron, Hewitt & Wasserman (1984). The original CCD data of Trager, Djorgovski & King (1993) were not available for our study. Due to the spread of the surface brightness data in the innermost part of the cluster different combinations of the data were used for the fit of the complete profile with the empirical density law of King (1962) applying the

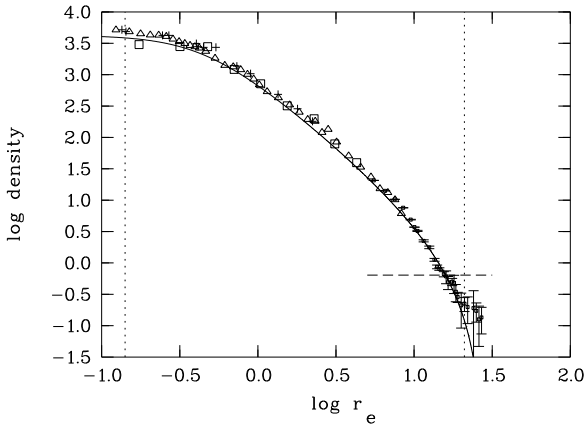

Fig. 2. Projected surface density profile of M 5. Logarithm of surface density in stars per arcmin^2 versus logarithm of the mean annulus radius r_e [arcmin]. The solid line shows the best fit with the empirical density law from King (1962). (Dots with error bars - star counts, triangles - Kron, Hewitt & Wasserman (1984); boxes - Kron & Mayall (1960), crosses - King (1966b); dashed line - background surface density). Only the star counts in combination with the surface photometry of King (1966b) in the interval between the dotted lines were used for the fit.

Levenberg-Marquardt-fitting-method (Press et al. 1992). Fig. 2 to Fig. 8 show the complete profiles of all measured globular clusters in logarithmic scale. The solid lines characterize the best representation of the data by King's density law.

The surface brightness profiles of the seven globular clusters are well represented by the empirical density law of King (1962). In the case of M 12, M 15 and NGC 5053 some inner surface brightness data ($r_e \leq 1$ arcmin) seem to lie systematically above or below the best fit values. These data points were omitted from the fitting to avoid a failure of the fitting procedure due to their large variation. The outer regions of M 5, M 12, M 13, M 15 and NGC 5466 could not be described by King's density law. They were also omitted in order to get a reliable fit of the complete profile.

Table 3 shows the derived parameters: tidal radius r_t, core radius r_c and the related concentration parameter of the examined globular clusters. Column (5) gives the reference for the data used in the final best fit.

For comparison we include the results of Trager, King & Djorgovski (1995) derived by fitting King's (1966a) dynamical density law in Table 4. In addition, column 5 gives the r_t values of Peterson & King (1975) resulting from conventional star counts. The empirical King model disagrees only for highly concentrated clusters ($c > 2.0$) with the dynamical density model. For our examined cluster we can directly compare the tidal radius r_t, the core radius r_c and the concentration parameter of both models. Our core radii r_c confirm the values of Trager and co-workers as expected from the correlation with the surface brightness data. The large error of r_c in the case of M 15 seems to arise due to the core collapsed nature of this cluster which we cannot determine on the basis of our data. The tidal radii

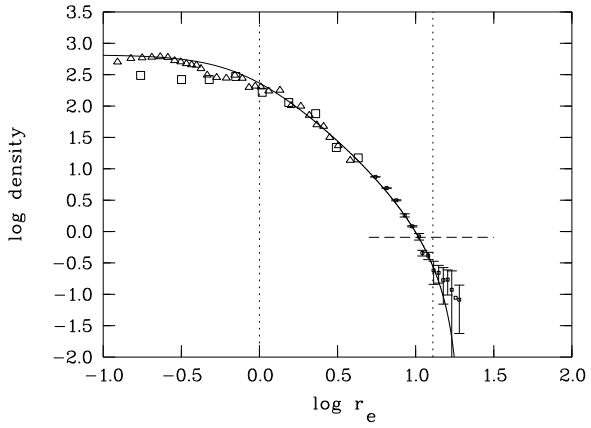

Fig. 3. Projected surface density profile of M 12 (cf. Fig. 2). Only the star counts (dots with error bars) in combination with the electronographical photometry of Kron, Hewitt & Wasserman (1984) (triangles) in the interval between the dotted lines were used for the fit.

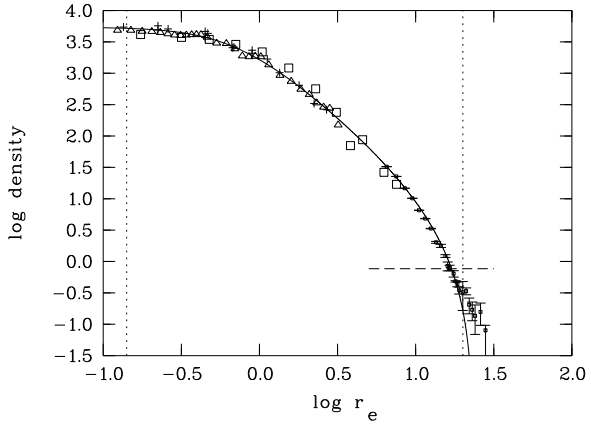

Fig. 4. Projected surface density profile of M 13 (cf. Fig. 2). Only the star counts (dots with error bars) in combination with the surface photometry of King (1966b) (crosses) in the interval between the dotted lines were used for the fit.

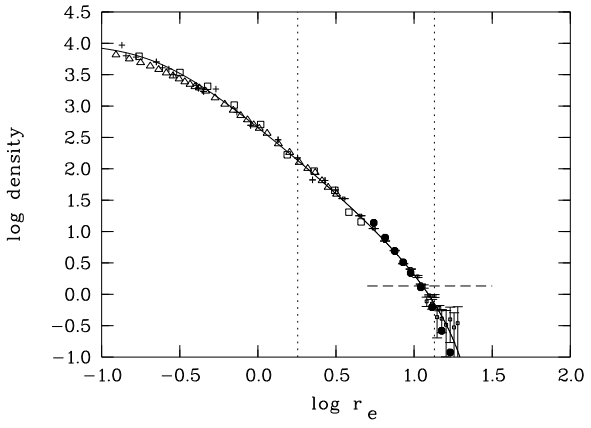

Fig. 5. Projected surface density profile of M 15 (cf. Fig. 2). Only the star counts (dots with error bars) in combination with the electronographical photometry of Kron, Hewitt & Wasserman (1984) (triangles) in the interval between the dotted lines were used for the fit. Filled circles represent the star counts of Grillmair et al. (1995).

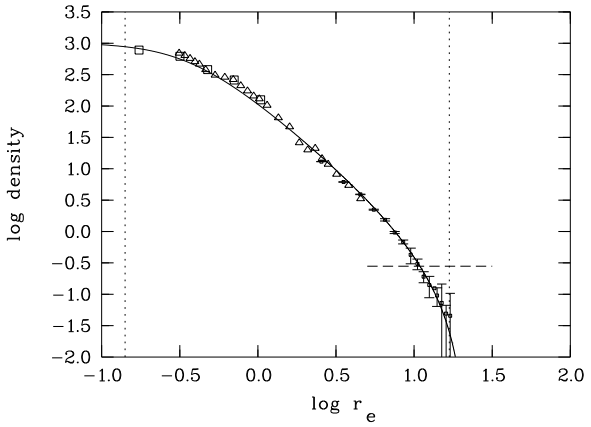

Fig. 6. Projected surface density profile of M 53 (cf. Fig. 2). Only the star counts (dots with error bars) in combination with the surface photometry of Kron & Mayall (1960) (boxes) in the interval between the dotted lines were used for the fit.

differ from the r_t values found by Trager and co-workers. For the clusters M 5, M 13, M 53, NGC 5053 and NGC 5466, our r_t values are 1-3 arcmin smaller than those of Trager, King & Djorgovski (1995), whereas the tidal radii of M 5, M 53 and NGC 5466 confirm the values of Peterson & King. There is no systematic trend of our derived tidal radii in comparison to the values obtained from conventional star counts. The large tidal radius r_t = 52.70 arcmin for NGC 5466 given in Table 4 is related to the uncertainty in the data indicated by the large error of the concentration parameter (Trager, King & Djorgovski 1995). Peterson & King (1975) have obtained a value of r_t = 20.89 arcmin. For M 15, Trager and co-workers could not derive r_t by fitting the non-core collapsed model of King (1966a). Our tidal radius of M 12 is about 3 arcmin larger than the value obtained by Trager and his collaborators.

The projected density profiles of M 5, M 12, M 13, M 15 and NGC 5466 reveal an increased surface density for $r_e > r_t$ which may be an indication of a tidal tail, caused by a halo of unbounded stars around these globular clusters, as recently discussed by Grillmair et al. (1995) for 12 Galactic globular clusters. The cluster M 15 belongs both to our sample and to that of Grillmair's group. The star counts of Grillmair et al. (1995), as shown in Fig.5, are consistent with our data. Althouth they obtained smaller densities for $\log r_e > 1.2$ the onset of the tidal tail starts at nearly the same density value (log density ≈ -0.5). This agreement could indicate the real nature of the tail. Fitting the King model to their

surface density in a radial range of 5.0 to 16.0 arcmin they obtained a tidal radius of r_t = 23.2 arcmin for M 15. In order

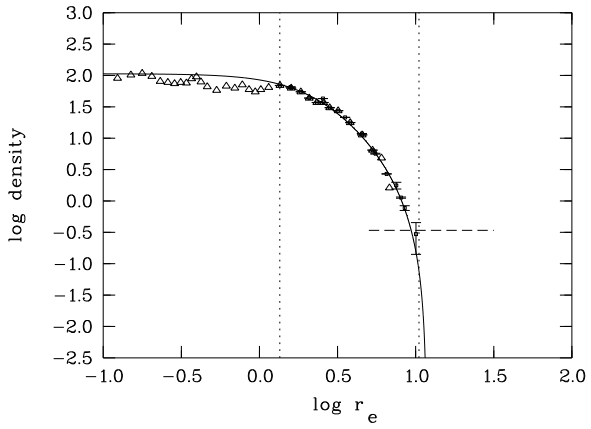

Fig. 7. Projected surface density profile of NGC 5053 (cf. Fig. 2). Only the star counts (dots with error bars) in combination with the electronographical photometry of Kron, Hewitt & Wasserman (1984) (triangles) in the interval between the dotted lines were used for the fit.

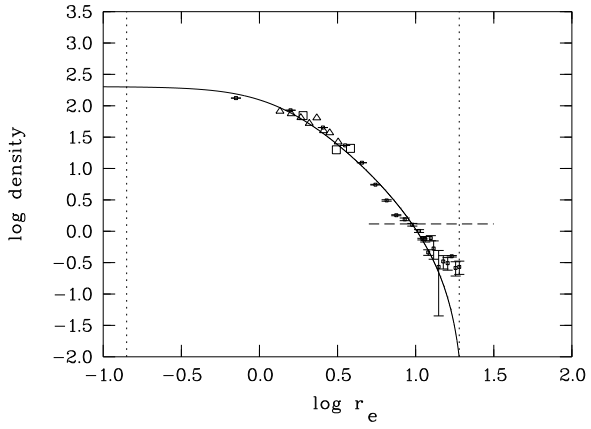

Fig. 8. Projected surface density profile of NGC 5466 (cf. Fig. 2). Only the star counts (dots with error bars) in combination with the electronographical photometry of Kron, Hewitt & Wasserman (1984) (triangles) in the interval between the dotted lines were used for the fit.

to get a reliable fit we used only the data up to a radius of 13.5 arcmin.

The strongest indication of a tidal tail can be seen in the density profiles of M 12, M 13 and NGC 5466 (Fig. 3, 4 and 8). The presence of a strong tidal tail in NGC 5466 would be consistent with the occurence of extra-tidal stars in NGC 5466 found by Pryor et al. 1991. From their studies of the velocity dispersion they assumed that NGC 5466 must have lost much of its original mass through stellar evaporation and tidal stripping.

Since our background examination is extended over large areas around the clusters we believe to have subtracted correct background values. A subtraction of too high background values would imply to get systematically lower tidal radii in comparison to the results of other authors. Nevertheless, it should be pointed out that from our results we cannot be confident in the evidence of the tidal tails. A more detailed two-dimensional study of the local background in the vicinity of the globular clusters (cf. Grillmair et al. 1995) will allow to determine the real nature of the tails.

The member counts derived by Kharchenko, Scholz & Lehmann (1996) do not indicate a tidal tail in the case of M 5. The discrepancy between the results may be due to the different magnitude limit of the member counts in comparison to the star counts.

Table 3. Derived structural parameters r_t, r_c and c.

object	r_t [arcmin]	r_c [arcmin]	c	ref.
NGC 5053	11.78±0.27	2.24±0.13	0.72±0.03	1,4
NGC 5466	20.98±0.57	1.32±0.05	1.20±0.02	1,4
M 5	27.93±0.80	0.44±0.04	1.79±0.04	1,3
M 12	19.30±0.43	0.77±0.07	1.40±0.04	1,4
M 13	23.79±0.10	0.68±0.01	1.54±0.01	1,3
M 15	27.05±0.95	0.22±0.23	2.08±0.45	1,4
M 53	21.87±0.53	0.35±0.01	1.79±0.02	1,2

1. automated star counts (this work)
2. aperture surface photometry (Kron & Mayall 1960)
3. aperture surface photometry (King 1966b)
4. electronographical photometry (Kron, Hewitt & Wasserman 1984)

Table 4. Structural parameters: literature values of Trager, King & Djorgovski (1995) for r_t, r_c and c (column 2-4) and of Peterson & King (1975) for r_t in column (5).

object	r_t [arcmin]	r_c [arcmin]	c	r_t (P.& K.) [arcmin]
NGC 5053	14.85	2.248	0.82±0.40	13.80
NGC 5466	52.70	1.958	1.43±0.60	20.89
M 5	29.64	0.400	1.87±0.20	28.84
M 12	15.92	0.664	1.38±0.20	18.20
M 13	27.04	0.875	1.49±0.20	26.92
M 15	-	0.068	2.50±0.20	20.89
M 53	22.48	0.373	1.78±0.20	21.87

5. Conclusions

Automated star counts of seven Galactic globular clusters on Schmidt plates from the Tautenburg, Palomar and UK telescopes have been used in order to obtain the complete projected density profiles of the clusters in correlation with surface brightness profiles of different authors. We used a new luminosity-dependent crowding correction and special account was given to a reliable background subtraction. Fitting the empirical density law of King (1962), we derived the tidal radius r_t, the core radius r_c and the concentration parameter c for the following clusters: M 5, M 12, M 13, M 15, M 53, NGC 5053 and NGC 5466.

Due to the higher statistical significance of our data in the outer cluster region we increased the accuracy of the tidal radii in comparison to the conventional star counts of Peterson & King (1975).

For the globular clusters NGC 5466, M 5, M 12, M 13, M 15 we have found some indication for tidal tails, caused by a halo of unbounded stars around the cluster, as described by Grillmair et al. (1995) in their examination of 12 Galactic globular clusters. Recently Grillmair et al. (1996) found evidence for tidal tails in two out of four clusters examined in M31, confirming the existence of tidal tails of globular clusters in other galaxies. To verify the nature of the tails in our cases, further investigations including a region around the clusters (cf. Grillmair et al. 1995) is needed.
Our star counts data will be available via email request under ilehmann@aip.de.

Acknowledgements. We would like to thank K.-H. Schmidt, N. Junkes and S. Friedrich for their constructive discussions and the careful reading of the manuscript. Also we thank the Tautenburg, Palomar and UKST Observatories for supplying the plates and Mike Irwin for measuring them on the APM. Last but not least we want to thank the referee C.J Grillmair for his valuable comments.

References

Arp H., 1955, AJ, 60, 317
Arp H., 1962, ApJ, 135, 311
Cuffey J., 1965, AJ, 70, 732
Bunclark P.S., Irwin M.J., 1983, in Rolfe E.J., ed, Proc. of Internat. Colloq. on Statistical Methods in Astronomy, ESA SP-201, p.195
Baum W.A., Hiltner W.A., Johnson H.L., Sandage A.R., 1959, ApJ 130, 749
Da Costa G.S., Freeman K.C., 1976, ApJ, 206,128
Djorgovski S., King I.R., Vuosalo C., Oren A., Penner H., 1986, in Instrumentation and Research programmes for small telescopes, IAU Symp. 118, eds. J. Hearnshaw & P. Cottrell, (Dordrecht: A. Reidel) p. 281
Grillmair C.J., Ajhar E.A., Faber S.M., Baum W.A., Holtzman J.A., Lauer T.R., Lynds C.R., O'Neil E.J., Jr., 1996, AJ, 111, 2293
Grillmair C.J., Freeman K.C., Irwin M., Quinn P.J., 1995, AJ, 109, 2553
Herzog A.D., Illingworth G.D., 1977, ApJ Suppl. Ser., 33, 55
Irwin M., 1985, MNRAS, 214, 575
Irwin M., Trimble V., 1984, AJ, 89, 83
Kharchenko N., Scholz R.-D., Lehmann I., 1996, A & AS, in press
Kibblewhite E., Bridgeland M., Bunclark P., Cawson M., Irwin M., 1984, in Capaccioli M., ed, Proc. of Conference on Astronomy with Schmidt-Type Telescopes, Reidel Publ., p. 89
King. I.R., 1962, AJ, 67, 471
King. I.R., 1966a, AJ, 71, 64
King. I.R., 1966b, AJ, 71, 276
King. I.R., Hedemann E.,Jr., Hodge S.M., 1968, AJ, 73, 456
Kron G.E., Hewitt A.V., Wasserman L.H., 1984, PASP, 96, 198
Kron G.E., Mayall N.U., 1960, AJ, 65, 581
Lindgren B.W., 1962, Statistical Theory (Macmillan, New York), p. 268
Nemec J.M., Harris H.C., 1987, ApJ, 316, 172
Peterson C.J., King I.R., 1975 AJ, 80, 427
Press H.W., Teukolski S.A., Vetterling W.T., Flannery B.P., 1992, Cambridge Press, Numerical Recipes in FORTRAN, sec. edition
Pryor C., McClure R. D., Fletcher J. M., Hesser J. E., 1991, AJ, 102, 1026
Racine R., 1971, AJ, 76, 331
Richer H.B., Fahlman G.G., 1989, ApJ, 339, 178
Sandage A., 1970, ApJ, 162, 841
Sandage A., Katem B., 1977, AJ, 82, 389
Sato T., Richer H.B., Fahlman G.G., 1989, AJ, 98, 1335
Scholz R.-D., Odenkirchen M., Hirte S., Irwin M., Börngen F., Ziener R., 1996, MNRAS, 278, 251
Scholz R.-D., Odenkirchen M., Irwin M. 1993, MNRAS, 264, 579
Scholz R.-D., Odenkirchen M., Irwin M., 1994, MNRAS, 266, 925
Trager S.C., Djorgovski S., King I.R., 1993, ASP Conf. Ser., 50, 347
Trager S.C., King I.R., Djorgovski S., 1995, Aj, 109. 218

This article was processed by the author using Springer-Verlag LaTeX A&A style file *L-AA* version 3.